Testing an Urban Climate Simulator

GEOLOGICAL SURVEY PROFESSIONAL PAPER 1099–E

Testing an Urban Climate Simulator

By GORDON M. GREENE

THE INFLUENCES OF LAND USE AND LAND COVER IN CLIMATE ANALYSIS

GEOLOGICAL SURVEY PROFESSIONAL PAPER 1099-E

An example of environmental analysis using land use and land cover information

UNITED STATES GOVERNMENT PRINTING OFFICE, WASHINGTON : 1980

UNITED STATES DEPARTMENT OF THE INTERIOR

CECIL D. ANDRUS, *Secretary*

GEOLOGICAL SURVEY

H. William Menard, *Director*

Library of Congress Cataloging in Publication Data
Greene, Gordon M.
The influences of land use and land cover in climate analysis.
(Geological Survey professional paper; 1099-E)
Bibliography: p.
Supt. of Docs. no.: I 19.16:1099-E
1. Urban climatology—Mathematical models. 2. Land use, Urban—Environmental aspects—Mathematical models. I. Title. II. Series: United States. Geological Survey. Professional paper; 1099-E.
QC981.7.U7G73 551.6'9'1732 79-607092

For sale by the Superintendent of Documents, U.S. Government Printing Office
Washington, D.C. 20402

CONTENTS

ILLUSTRATIONS

TABLES

LIST OF ABBREVIATIONS AND SYMBOLS

ALB average shortwave albedo for all surfaces.

BAL_{t-1} the sum of R_n, S, H, and LE based on the second surface temperature estimate $(t-1)$.

BAL_{t-2} the sum of R_n, S, H, and LE based on the first surface temperature estimate $(t-2)$.

BEAM direct shortwave radiation flux, in watts per square meter.

CBD Central Business District land use category.

CITY subroutine in the URBD model which computes the soil damping depth (z_G).

COMM commercial area land use category.

C_p specific heat of air at constant pressure.

CPATH solar geometry input to the URBD model.

E_p saturation vapor pressure.

EPHEM subroutine in the URBD model which computes the solar declination.

EXT shortwave radiation flux on a horizontal surface outside the Earth's atmosphere.

F artificial heat flux due to combustion.

H kinetic or sensible heat flux into the atmosphere.

HDR high density residential land use category.

HEM diffuse shortwave radiation flux.

J Joule.

L latent heat of vaporization.

LDR low density residential land use category.

LE latent energy used in evapotranspiration.

MDR medium density residential land use category.

PARKS park land area land use category.

Q_{air} specific humidity of the air.

Q_{surf} specific humidity at the ground surface.

READIN geographical and meteorological input data to the URBD model.

RH relative humidity.

Ri bulk Richardson number.

$R_{lw}\uparrow$ longwave radiation emitted by the Earth's surface.

$R_{lw}\downarrow$ longwave radiation emitted by the Earth's atmosphere.

R_n radiation balance at the terrestrial surface (net radiation).

$R_{sw}\uparrow$ solar shortwave radiation reflected by the Earth's surface.

$R_{sw}\downarrow$ solar shortwave radiation incident upon the Earth's surface.

RUNTRI subroutine in the URBD model used to determine the condition of the soil temperature profile.

S net heat flux to buildings, roads, and substrate.

SECANT algorithm used in the URBD model to compute a new surface temperature estimate, in order to stabilize the soil temperature profile.

SHDRAT shadow ratio.

SIG Stefan-Boltzman constant.

SILRAT silhouette ratio.

SKY area of a ground observer's sky hemisphere, in percent.

SOLURB subroutine in the URBD model which computes the shortwave radiation input.

SRHF surface relative humidity fraction.

SUN backscattered radiation flux on a horizontal surface at the Earth's surface.

T_{air} air temperature, in degrees Celsius.

T_C control run temperature of the URBD model for each land use type.

TERRAIN total shortwave radiation flux averaged over the urban surface.

T_m mean diurnal air temperature, in degrees Celsius.

T_{max} maximum temperature, in degrees Celsius.

T_{min} minimum temperature, in degrees Celsius.

T_{new} model computed surface temperature, based on manually derived high- and low-surface temperature estimates.

TRANS transportation land use category.

TSKY radiation temperature of the sky hemisphere.

T_{surf} surface temperature, in degrees Celsius.

T_{t-1} second surface temperature estimate, used in the URBD model to stabilize the soil temperature profile.

T_{t-2} first surface temperature estimate, used in the URBD model to stabilize the soil temperature profile.

T2 temperature at the first node below the ground surface, in degrees Celsius.

UBAL subroutine in the URBD model which computes R_n, S, H, and LE.

UPRIG subroutine in the URBD model which computes the amount of radiation on a vertical surface.

VERT total shortwave radiation on a vertical surface, in watts per square meter.

b_{ALB} slope, or b value, computed in the Student's t-test, of the albedo parameter.

b_{SILRAT} slope or b value, computed in the Student's t-test, of the silhouette ratio parameter.

b_{SRHF} slope, or b value, computed in the Student's t-test, of the surface relative humidity fraction parameter.

b_{z_o} slope, or b value, computed in the Student's t-test, of the surface roughness parameter.

b_1 slope of a specified regression line.

h_o obstacle height, in centimeters.

k von Karman's constant (0.4).

p atmospheric pressure, in millibars.

r coefficient of correlation.

t the period of a specified temperature fluctuation.

W watt.

z height above, or depth below, surface.

z_d atmospheric damping height, in centimeters.

z_G soil damping depth, in centimeters.

z_o surface roughness length, in centimeters.

Δz the change in height above, or depth below, surface, in centimeters.

κ thermal diffusivity, in square centimeters per second.

λ thermal conductivity, in Joules per centimeter per second per degree Celsius.

μ wind speed at height z, in centimeters per second.

ρ air density, in grams per cubic centimeter.

TESTING AN URBAN CLIMATE SIMULATOR[1]

By GORDON M. GREENE[2]

ABSTRACT

Geographic data, generally in the form of terrain information, are a primary input to urban climate simulation models. Five urban terrain parameters: silhouette ratio, substrate diffusivity, obstruction height, surface relative humidity fraction, and albedo account for most of the geographic input. In a test of the sensitivity of model-predicted surface temperatures to simulated changes in the five urban terrain parameters, the influences of these parameters on the urban thermal regime of Baltimore, Md., were analyzed. Results indicated that changes on the order of 30 percent, in individual urban terrain parameters, have relatively little effect on surface temperatures. When more than one of these parameters are considered together, however, changes within the ±30 percent range become more significant. The major benefit of the urban climate model in this analysis is not as a predictive tool, but as a method whereby relationships between input components are examined.

INTRODUCTION

The use of the energy-balance relationship to explain the partitioning of shortwave and longwave radiation at the Earth's surface can be deceptively simple. Stated in an equation:

> Net radiation=heat conducted into the ground+turbulent transfer of heat by (1) convection and evaporation.

Traditionally, the ideal setting for such a model of reality is an infinite, smooth plain with unvarying wind speed, air temperature, relative humidity, and solar radiation flux.

In contrast, consider this ideal against the reality of a few square blocks near the center of a large city. Streets are lined with multistory buildings, one side warmed by the early morning sun, the other side retaining the nighttime coolness. One block holds a small park with asphalt tennis courts, a large fountain used for wading, and a number of large old trees. A small shopping area is separated from the park by a four-lane street, busy with commuters. The shops are mostly two stories, some with freshly tarred roofs. A study of the energy balance relationship of such an area requires an accounting of the tremendous variety in structures, their materials, shapes, sizes, and orientations. Myrup (1969) and Outcalt (1972a, b) were among the first to quantify some of these variables, frequently referred to as urban terrain parameters, and incorporate them into urban simulation models.

The purpose of this report is to examine the influences of five urban terrain parameters: silhouette ratio, substrate diffusivity, obstruction height, surface relative humidity fraction, and albedo, on the urban thermal regime. The analysis is based on a test of the sensitivity of model-predicted surface temperatures to simulated changes in the five parameters. The simulation analysis was made in accordance with conditions existing in Baltimore, Md., on May 11, 1972. Land use and land cover data, from which values for the terrain parameters could be obtained, as well as thermal infrared images, against which the model could be verified, were available for that date in Baltimore.

REVIEW OF URBAN CLIMATE MODELING

Historically, the first major step in the study of urban climate relations was the recognition that large cities often have higher air temperatures in the city center than at the suburban fringes. This phenomenon was termed the "heat-island" effect and has been well described in the literature (Bornstein, 1968; Terjung, 1970).

The temperature differences between urban and rural areas result from numerous factors. Thermal characteristics of steel, concrete, and asphalt promote higher heat absorption and storage. A city center has a large proportion of vertical surfaces intercepting shortwave and longwave radiation. The atmospheric composition may be modified by more dust and aerosols over a city (Tuller, 1973). Rain in cities is usually drained away soon after falling, removing the possibility of net solar radiation being

[1] The research reported herein was funded in part by the National Aeronautics and Space Administration and U.S. Geological Survey as one phase of the Central Atlantic Regional Ecological Test Site (CARETS) Project.

[2] Department of Geography, University of Michigan, Ann Arbor, Mich.

used for evaporation (Hage, 1975). Finally, human activities in cities produce heat from a large number of sources.

As urban climate investigations became more sophisticated, increasing emphasis was placed on explaining differences in microclimates within the city proper (Terjung and others, 1970). Those factors which distinguish an urban area from the countryside are not spatially homogeneous and may, therefore, be studied as a function of land use (Outcalt, 1972a). Alexander and others (1976), suggest that the concept of an urban heat island may exist only as a function of faulty research methodology. For example, the use of street-level spot observations taken from a car may smooth out microclimate diversity within a city, if the immediate influence of a street on surface temperatures is stronger than that of the surrounding environment. In effect, the overall "texture" of an urban surface is so varied that the concept of a representative site for different land uses is meaningless. The only realistic approach, therefore, is to use area-averaging parameters (Myrup and Morgan, 1972; Marotz and Coiner, 1973).

The increasing use of remotely sensed thermal data provides the synoptic view of urban climates that early investigators were attempting to create. The ability to analyze the microclimate at a specific point and height above the ground is sacrificed, however, since the remotely sensed thermal image is a two-dimensional projection of a three-dimensional surface. Even so, the temperature field shown for a remotely sensed area is a unique value caused by the complex interaction of solar radiation with the particular geometric and thermal properties of that area. As demonstrated by Outcalt (1972a), remotely sensed data can be used to categorize land use and land cover, and the interaction of land use and land cover with climatic variables.

One method for studying this interaction is through computer modeling, which simulates the events assumed to be taking place. Models applied to urban climates are generally classified as attempts to study either mesoscale or microscale interactions (Schneider and Dickinson, 1974). Mesoscale models usually operate in two dimensions and are used to investigate the nature of the urban boundary layer. Emphasis is placed on those factors which alter the turbulent transfer processes for heat, moisture, and momentum over an urban area, similar to a micrometeorologist studying the changes in turbulence caused by the transition from a grassy field to an asphalt runway (see, for example, Gutman and Torrance, 1975; Leahey and Friend, 1971; McElroy, 1973; and Bornstein, 1975).

The approach used in this study relies on a microscale one-dimensional energy balance model pioneered by Myrup (1969). His first model has since been expanded for application to Ann Arbor, Mich., (Outcalt, 1972a) and Baltimore, Md. (Alexander and others, 1976). Myrup's original work also has been expanded and applied in a detailed study to Sacramento, Calif. (Myrup and Morgan, 1972).

The use of the model is helpful in studying urban climates because of the complexity of the city atmospheric interaction. Another benefit of this simulation model is that it allows one to link relationships which are only empirically justifiable to those processes which are well understood. The model provides the framework for arranging the information one has available as a system.

ENERGY BALANCE SIMULATION IN URBAN ENVIRONMENTS

The underlying principle of the surface energy balance in equation 1 is the conservation of energy. In a steady-state condition, the amount of energy gained must equal the amount of energy lost. Change is thought of as an instantaneous change to a new steady state. For urban applications, equation 1 can be rewritten as:

$$R_n+F=LE+H+S, \quad (2)$$

where:

R_n = radiation balance at the terrestrial surface (net radiation).
F = artificial heat flux due to combustion
LE = latent energy used in evapotranspiration
H = kinetic or sensible heat flux into the atmosphere
S = net heat flux to buildings, roads, and substrate.

Following convention, the energy flux for any term is considered positive if directed toward the surface, negative if directed away. Although many authors have used F as a component of the energy relationship (for example, Gutman and Torrance, 1975; Myrup, 1969), it was not included in this model since there are not enough data to give a meaningful artificial heat flux value to the different land uses. It is not clear if this is a significant omis-

sion. Yu and Wagner (1975) estimated F as 140 W/m^{-2} for New York City on a clear winter day with an air temperature of 0° C. A more reasonable estimate for May would be the estimate of heat flux due to vehicular activity of 7 W/m^{-2}, although air conditioning should also be considered. Both these heat fluxes are much smaller than the mean midday flux of longwave and shortwave radiation of 870 W/m^{-2}.

By specifying the boundary conditions, one can compute the energy flux contributed by each of the four energy balance components from the following assumptions and procedures. While each component can be expressed as a function of surface temperature, it is not possible to analytically solve equation 2 for the unique equilibrium surface temperature which balances the equation. One can, however, use either an analog model or a numerical iteration scheme to find the surface temperature.

The appendix to the Baltimore study (Alexander and others, 1976) contains a good summary of the derivations for each of the energy flux components. Rather than repeating those equations, this section presents the components in their finite-difference form for use in a digital computer model and explains the modifications used to adapt the energy balance relation to a city. In addition, this section examines the response of the energy flux components in the urban terrain parameters.

The first component, net radiation (R_n), can be broken down into its shortwave and longwave forms:

$$R_n + (R_{sw}\downarrow - R_{sw}\uparrow) + (R_{lw}\downarrow - R_{lw}\uparrow) \quad (3)$$

where $R_{sw}\downarrow$ is the solar shortwave radiation incident upon the Earth's surface, $R_{sw}\uparrow$ is the solar shortwave radiation reflected by the Earth's surface, $R_{lw}\downarrow$ is the longwave radiation emitted by the Earth's atmosphere, and $R_{lw}\uparrow$ is the longwave radiation emitted by the Earth's surface.

Looking at the shortwave equation:

$$R_{sw}\downarrow - R_{sw}\uparrow = [(1 - ALB) \times (1 - SHDRAT) \times (BEAM + HEM)] + (SHDRAT \times HEM) + (SILRAT \times VERT) \quad (4)$$

where:

ALB=average shortwave albedo for all surfaces

$SHDRAT$=shadow ratio (discussed below)

$BEAM$=direct shortwave radiation flux

HEM=diffuse shortwave radiation flux

$SILRAT$=silhouette ratio (discussed below)

$VERT$=total shortwave radiation on a vertical surface.

The definition of the urban terrain parameter $SILRAT$ is illustrated in figure 1. The role $SILRAT$ plays as a roughness factor is shown in figure 2. The average height of obstructions for a particular area, or for a particular land use, is represented by h_o. As building density increases (fig. 2A to B), the total amount of incident shortwave radiation per unit ground area also increases. Figure 2C is included to show that past a certain critical value of $SILRAT$, the amount of incident shortwave radiation will decrease as the density increases. The increase in shadowed area with larger zenith angles is roughly approximated by:

$$SHDRAT = [1 - \cos(\text{zenith angle})]^{3}. \quad (5)$$

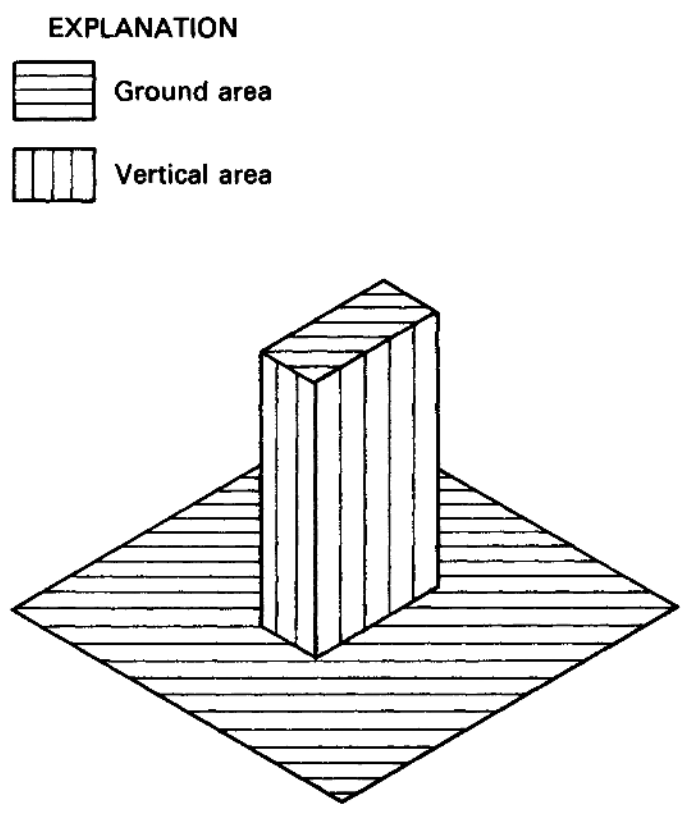

FIGURE 1.—$SILRAT$, where $SILRAT = \frac{\text{vertical area}}{\text{ground area}}$.

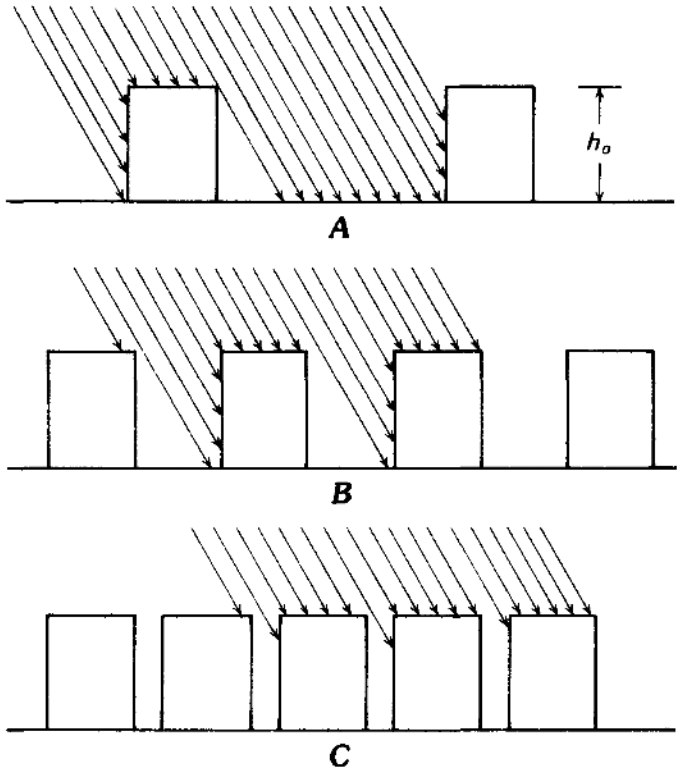

FIGURE 2.—The interception of direct shortwave radiation by buildings.

The net longwave radiation is computed as:

$$R_{lw}\downarrow - R_{lw}\uparrow = [(1-SILRAT)\times SIG\times TSKY^4] + [(SILRAT-1)\times SIG\times T_{surf}^4], \quad (6)$$

where SIG is the Stefan-Boltzman constant and $TSKY$ is the apparent radiant temperature of the sky hemisphere. Emissivity is assumed to be 1. In this case, $SILRAT$ is used as a value roughly equivalent to a variable called the view factor, defined as that portion of radiation leaving a surface that is intercepted by another surface. A representative sky hemisphere, as "seen" from a point radiation source, is illustrated in figure 3*A*. This radiation source is located at point *a* in figure 3*B*. Note, however, that the value of the view factor could change somewhat depending on the position of *a* in figure 3*B*, while $SILRAT$ would remain constant. The approximation is used only in the absence of actual values for the view factor.

The two terms that contribute to turbulent heat transfer are each computed using analogous relationships. Sensible heat flux to the air can be calculated as:

$$H = \frac{k^2\rho\mu C_P}{(\ln(z_d/z_0))}\ 2\times|(1-18\times Ri)^{1/4}|\times(T_{air}-T_{surf}). \quad (7)$$

Evaporative heat loss is similar:

$$LE = \frac{k^2\rho\mu L}{(\ln(z_d/z_0))}\ 2\times|(1-18\times Ri)^{1/4}|\times(Q_{air}-Q_{surf}), \quad (8)$$

where:

k = von Karman's constant (0.4)
ρ = atmospheric pressure
μ = wind speed at height z
C_p = specific heat of air at constant pressure
z_d = atmospheric damping height (discussed below)
z_0 = surface roughness length (discussed below)
Ri = bulk Richardson number
T_{air} = air temperature
T_{surf} = surface temperature
Q_{air} = specific humidity of the air
Q_{surf} = specific humidity at the ground surface
L = latent heat of vaporization.

In general, wind speeds are slower near the ground than they are away from the surface due to the drag exerted on moving air by the ground surface. When temperatures are nearly constant with height, wind speed increases linearly with the natural logarithm of the height (Sellers, 1965). If one assumes some layer of air close to the ground, across which heat is transferred solely by molecular processes, it is possible to imagine a non-zero height, z_0, at which the wind speed is zero. This height is called the roughness length.

Presumably, as the surface texture gets rougher, the lower surface of the boundary layer rises due to turbulence, and the height at which the wind speed is zero also rises. The height above which the effect of the surface roughness is no longer felt, the atmospheric damping height, is represented by z_d.

The logarithmic relationship between z_d, z_0, and μ has been derived from observations over uniform flat surfaces to a height of about 20 m (Sellers, 1965). Under these conditions, z_0 can be derived as the y-intercept of the log-law relation. Since the assumption of a uniform surface is clearly violated in urban areas, Lettau suggested an approximation of z_0 as a function of the average height of obstructions and the silhouette ratio (Lettau, 1969):

$$z_0 = 0.5\times h_0\times SILRAT \quad (9)$$

He also notes that the parameter $SILRAT$ loses

validity as it approaches unity. Like *SILRAT*, the use of z_o can be abused in extreme conditions. Looking again at figure 2, it is clear that, as the buildings crowd closer together, there will be a point when the roof tops function as the new ground surface and z_o goes back toward 0.

The second factor in equations 7 and 8 corrects for the unstable air conditions occurring throughout most of a diurnal cycle. The bulk Richardson number, *Ri*, in this adiabatic correction function is computed by Sellers (1965) as:

$$Ri=\frac{(980/T_{air})\times[(T_{air}\ T_{surf})/\ln(z_d/z/z_0)]}{[\mu/\ln(z_d/z_0)]^2} \quad (10)$$

The urban terrain parameter *SRHF*, the surface relative humidity fraction, is used to compute the specific humidity at the surface:

$$Q_{surf}=\frac{.622\rho\times E_P\times SRHF}{\rho-E_P}, \quad (11)$$

where E_p is the saturation vapor pressure. Myrup (1969) used the surface relative humidity fraction, *SRHF*, instead of surface relative humidity because of the heterogeneous nature of a given urban area. Since the surface relative humidity is considered to be 100 percent when the soil contains enough water, Myrup calculated *SRHF* by finding the relative proportion of an area covered by freely transpiring vegetation.

To calculate the soil heat flux, the model solves

$$S=\lambda/\Delta z\times(T2\ -\ T_{surf}), \quad (12)$$

where λ is the thermal conductivity and Δz is the change in depth. In this model, eight nodes are used to compute the soil temperature profile. The surface node is T_{surf}, and $T2$ is the ground temperature at the first node below the surface, set at 5 cm in this study. The program uses an implicit solution to a thermal diffusion equation to update the soil temperature profile based on a method suggested by Outcalt and Carlson (1975).

Thermal conductivity is not an input parameter due to the diverse surfaces and materials in any one land use. Instead, thermal diffusivity, κ, is calculated as a function of *SRHF* by scaling κ between the diffusivity of dry concrete (0.02 $cm^2\ sec^{-1}$) and wet soil (0.005 $cm^2\ sec^{-1}$).

$$\kappa=(SRHF\times 0.005)+[(1-SRHF)\times 0.02]. \quad (13)$$

The assumption is that as the *SRHF* becomes smaller, the percentage of surface covered by concrete becomes larger, and the value of κ approaches the κ of concrete (Outcalt, 1972a). Thermal conductivity is found as the product of κ and an average heat capacity of 0.21 J cm^{-3} (Sellers, 1965).

Equations 2 through 13 may now be used to estimate the effects of changes in the urban terrain parameters, silhouette ratio, height of obstructions, surface relative humidity fraction, shortwave albedo, and thermal diffusivity on the surface temperature.

The variable *SILRAT* is used in the computation of R_n, H, and LE. As *SILRAT* increases, $R_{lw}\downarrow - R_{lw}\uparrow$ becomes less negative, making R_n larger. In equation 4, an increase in *SILRAT* also increases the amount of energy intercepted on vertical sur-

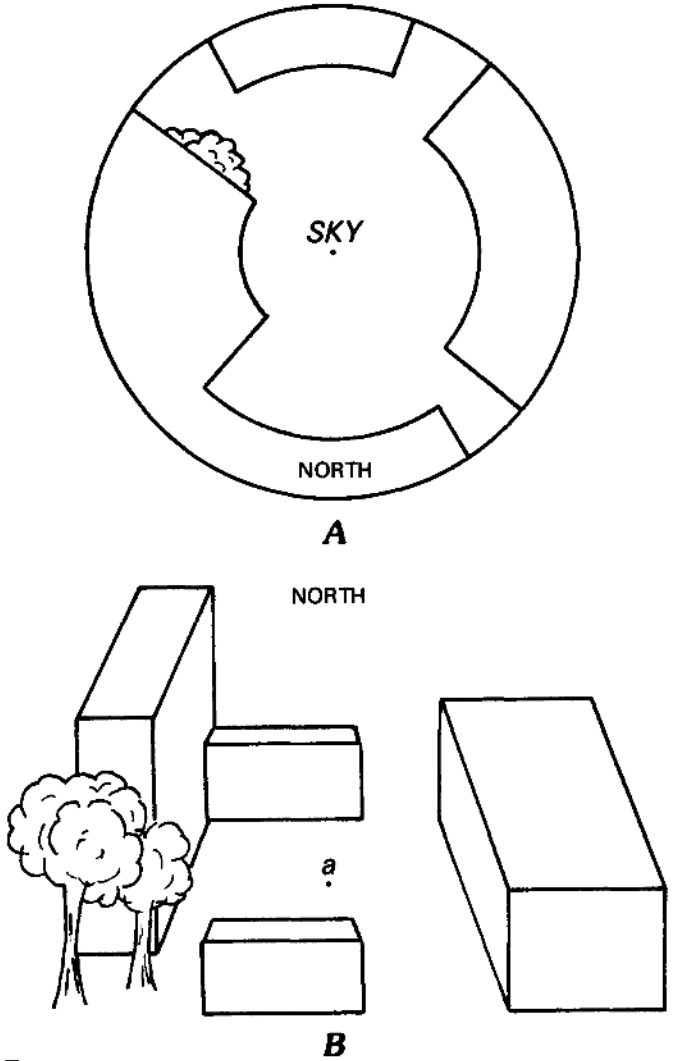

FIGURE 3.—The interception of longwave radiation by buildings and vegetation (adopted from Myrup and Morgan, 1972). *A*, Sky hemisphere view from point *a*; view factor-(1−*SKY*)/total area. *B*, Site view.

faces, further increasing R_n. If all other variables are held constant, T_{surf} will increase.

SILRAT also affects H and LE on the opposite side of the equal sign in equation 2 because it is used to compute z_o. An increase in z_o increases the turbulent exchange coefficient, the first factor in equation 7. The value of the second factor, the adiabatic correction for unstable air, also will increase but at a much slower rate.

The overall effect of an increased z_o will be to magnify the direction of flux as determined by T_{air}–T_{surf}. For example, if T_{surf} is larger than T_{air}, an increased z_o will cause H to become more negative. With all else held constant, a stronger H away from the surface will cause T_{surf} to drop.

Similarly, an increased z_o increases the magnitude of LE, with the sign depending on the relation Q_{air}–Q_{surf}. It would be possible to have the signs of Q_{air}–Q_{surf} and T_{air}–T_{surf} such that an increased z_o would magnify LE away from the surface but increase H toward the surface.

Equation 9 shows that h_o, the height of obstructions, is linearly related to z_o. One would expect an increase in h_o to have the same effect on H and LE as a comparable increase in *SILRAT* if R_n was held constant. Note that an increased h_o would not create an increased vertical surface area since *SILRAT* is input separately.

The effects of changes in *ALB* and κ are the most transparent of all the parameters. An increase in *ALB* causes $R_{sw}\downarrow - R_{sw}\uparrow$ to decrease and the value of T_{surf} must, therefore, decrease to compensate. Equation 12 demonstrates that an increased λ would increase the magnitude of the soil heat flux. For example, at midday T_{surf} is much higher than $T2$. An increased λ would increase the heat flux into the ground and cause T_{surf} to drop if all else were constant. The thermal profile would also adjust more quickly to changes at the surface since the speed of diffusion has increased.

The parameter *SRHF* affects both LE and S. As equation 13 shows, an increase in *SRHF* decreases the value of κ which lowers the magnitude of S. The value of Q_{surf} in equation 11 is also determined by *SRHF* being affected by it linearly. The relative magnitude of Q_{surf} then determines whether the flux of evaporation increases or decreases. For example, an increase in *SRHF* would force LE to become more negative if Q_{surf} was larger than Q_{air}, forcing T_{surf} to decrease.

Of the five urban terrain parameters, only changes in *ALB* cause predictable changes in surface temperature. In all other cases, the direction of the component flux is a function of the sign of the temperature or specific humidity difference. In the case of *SILRAT*, h_o, and *SRHF*, more than one component is adjusting to the change.

THE MODEL

The model used for this study is based on a surface-energy budget simulator developed by Outcalt and Carlson (1975). Their report describes in detail the structure of the program. This section generally outlines the model used, (URBD), and describes changes made to accommodate the urban influences on the energy-balance components as discussed in the last section.

If a city is considered as a mosaic of textures and materials, an urban model must differentially respond to the same meteorological conditions based on certain site characteristics. Outcalt's original study of land use effects (1972a) analyzes the responses of four land use types, each defined by the specification of three urban terrain parameters, surface relative-humidity fraction, obstruction height, and silhouette ratio.

For this study, albedo was added in order to accentuate the differences between heavily and lightly vegetated areas. In addition, roughness length was input instead of obstruction height since the data used to operate the model were provided in this form. This substitution is merely for convenience and does not affect the simulated temperature values since z_0 and h_0 are linearly related as shown in equation 9.

Other input variables include latitude of the site and the time of year, which are used to calculate the solar geometry. The density of dust particles in the air, and amount of precipitable water to calculate the amount of shortwave radiation transmitted through the atmosphere, are also specified as input variables. Air temperature, atmospheric pressure, relative humidity, and wind speed are read into the model as the meteorological boundary conditions. As the model is currently written, these last four variables are specified for each time step the model is run, every hour in this case. The model in this form is referred to as the observed hourly input model. With slight modification in the input procedure, however, the model can also run on mean daily values for those variables using a wide range of time intervals. This form of the model is called the daily mean value input model.

The overall flow of the program is illustrated in figure 4. Notice that the model cycles through the

daily (24 hourly) data twice in order to stabilize the soil temperature profile before solving for the equilibrium surface temperature. Fed by a high guess and a low guess for the surface temperature, the *SECANT* algorithm computes a new guess with the following relationship:

$$T_{new}=T_{t-1}-\frac{[(T_{t-1}-T_{t-2})\times BAL_{t-1}]}{BAL_{t-1}-BAL_{t-2}}, \quad (14)$$

where T_{t-1} refers to the previous guess of the temperature and T_{t-2} refers to the guess prior to T_{t-1}. BAL is the current sum of R_n, S, H, and LE. The routine converges to $BAL=0\pm0.7\text{W/m}^{-2}$ usually within six iterations.

The subroutines used in the Outcalt and Carlson URBD model (1975) were not designed for city use, which necessitated some restructuring and modification. For example, the shadow generator, *SHDRAT*, has been included in subroutine *CPATH*, the solar geometrician. Subroutine *SOLURB*, which calculates shortwave radiation, does not allow the albedo to vary as a function of the angle of incidence. Such a refinement would not be justified since the albedo for any land use is an average for such diverse materials as roofs, vegetation, and concrete. Subroutine *RUNTRI* has also been simplified by disallowing variable porosity and thermal conductivity in the substrate. Instead, thermal diffusivity is assumed to take on values that can only range between the diffusivity of dry concrete (roughly 0.02 $\text{cm}^2\ \text{sec}^{-1}$) and that of wet soil (roughly 0.005 $\text{cm}^2\ \text{sec}^{-1}$).

It is necessary in this model to establish a lower boundary for the soil heat flux in order to simulate the diffusion of heat through the substrate at each time step. The damping depth, z_G, is calculated in subroutine *CITY* using the Terzaghi relationship (Outcalt and Carlson, 1975):

$$z_G=(12\times t\times\kappa)^{1/2}, \quad (15)$$

where t represents the period of the temperature fluctuation one is concerned with. In this case, one is dealing with diurnal variation so $t=4.32\times10^4$ sec (12 hours). Using the extremes of κ as endpoints, the range of z_G is between 51 cm and 102 cm.

APPLICATION OF THE MODEL

To test the response of the model to differing urban terrain characteristics, data were obtained from a project conducted by the U.S. Geological Survey (USGS) (Alexander and others, 1976). One of the principal goals of the USGS investigation was to evaluate how well thermal scanner data, collected by spacecraft, could be used for studying urban climates.

The data for this model analysis come from an early experiment in the USGS study. On May 11, 1972, the Environmental Research Institute of Michigan (ERIM) directed three aircraft flights over Baltimore, Md., at an altitude of approximately 1,500 m. The third ERIM run, flown between the hours of 1345 and 1415 e.d.t., provides the observed data used for the verification of the URBD model. The flight path is shown in figure 5, running across Baltimore from the northwest to the southeast.

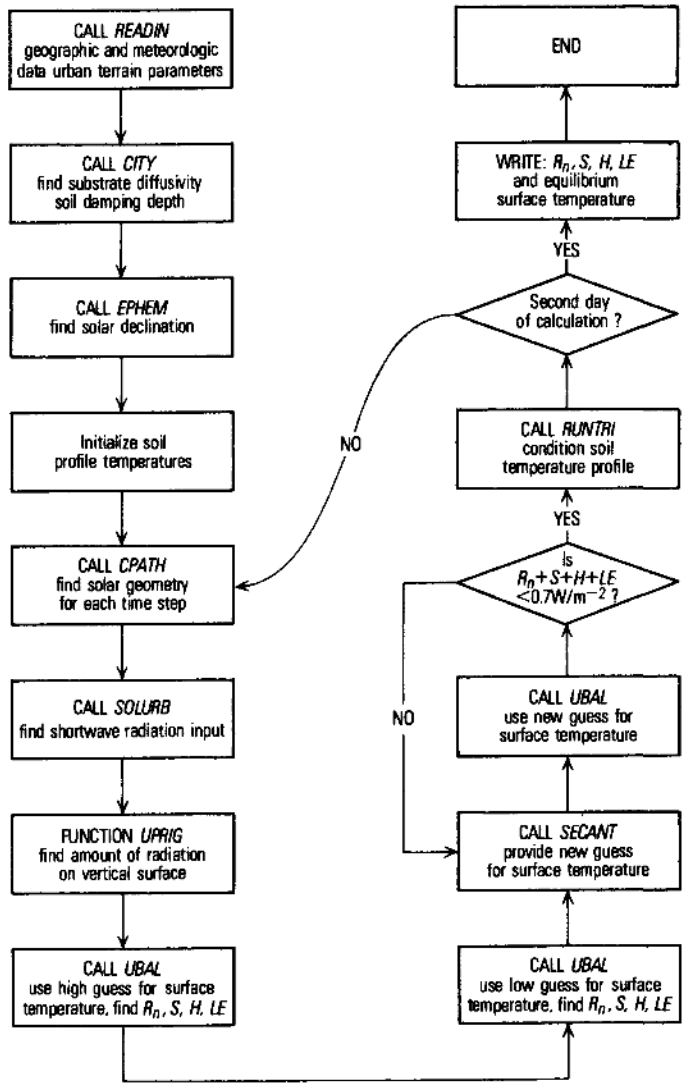

FIGURE 4.—Flow chart of the Outcalt and Carlson URBD model (1975).

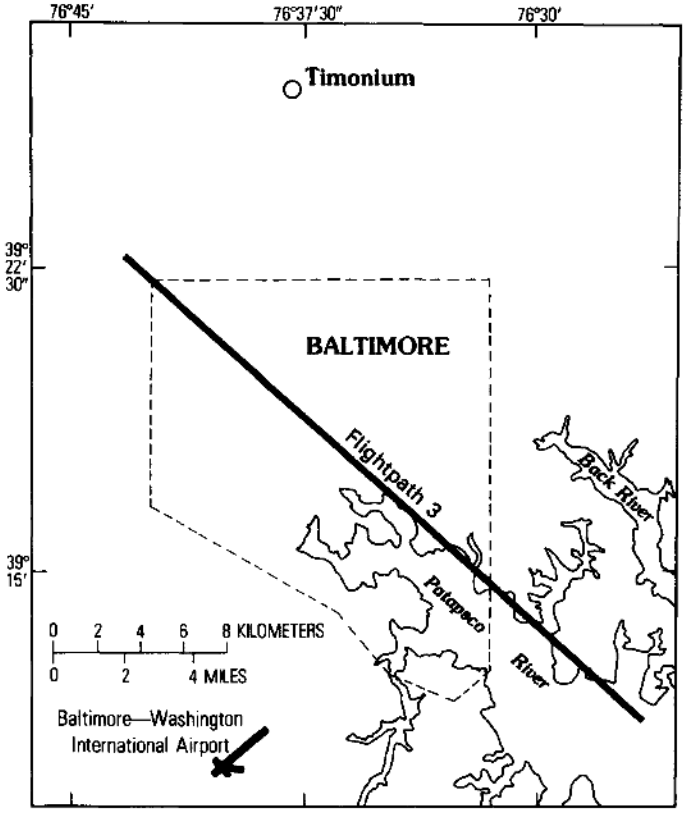

FIGURE 5.—Path of the third flight across Baltimore, Md., along which multispectral scanner data (including thermal) were obtained by the ERIM aircraft on May 11, 1972.

Weather records for May 11, 1972, show that the day was clear and cool with a steady breeze from the west. Temperature ranges for May 9–11, 1972, listed in table 1, support the observation that a cold front passed through the area on May 10, 1972, bringing a fairly homogeneous air mass over the Washington-Baltimore area (Alexander and others, 1976). Under these conditions, hourly meteorological observations from Baltimore-Washington International Airport, located eight miles southwest of Baltimore in the direction of Washington, are representative of the region. These hourly values of air temperature, wind speed, air pressure, and relative humidity are listed in table 2.

The principal advantage of the third May 11, 1972, flight, over the two flown earlier that day, is that it scanned an area with a high diversity of land use types. The effects of seven land uses on surface temperature were simulated in this study to give an idea of the possible range of microclimates within a city. These land uses are: low-density residential (*LDR*), medium-density residential (*MDR*), high-density residential (*HDR*), central business district (*CBD*), commercial (*COMM*), transportation (*TRANS*), and urban parks (*PARKS*). The urban terrain characteristics of these land use types are presented in table 3. Values of these parameters were determined early

TABLE 1.—*Recorded meteorological data*

[Washington, D.C.: T_{max} occurred at 1640 e.s.t., T_{min} occurred at 0515 e.s.t. Highest observed wind speed since 0800: 671 cm sec^{-1} at 1720 e.s.t. from west.
Source: "Washington Post," daily weather information, May 10–12, 1972]

	T_{max}(°C)	T_{min}(°C)	Precip. (cm)
Tuesday, May 9, 1972 (24 hours ending at 2000 e.s.t.)			
Baltimore	23	14	0.02
Washington, D.C.	23	16	.18
Wednesday, May 10, 1972 (24 hours ending at 2000 e.s.t.)			
Baltimore	12	10	2.11
Washington, D.C.	13	11	1.57
Thursday, May 11, 1972 (24 hours ending at 2000 e.s.t.)			
Baltimore	21	4	0.0
Washington, D.C.	23	7	.0

TABLE 2.—*Surface weather observations at Baltimore-Washington International Airport, May 11, 1972*

[Source: National Climate Center, National Oceanic and Atmospheric Administration, Asheville, North Carolina 28801]

Time (e.s.t.)	T_{air} (°C)	μ (cm sec^{-1})	P (mb)	RH (percent)
0055	7.2	360	1021	0.60
0155	7.8	309	1021	.56
0255	5.6	257	1021	.60
0355	5.6	257	1021	.60
0455	4.4	309	1021	.64
0555	5.0	257	1022	.67
0655	8.3	206	1023	.65
0755	12.8	309	1023	.55
0855	15.0	515	1023	.41
0955	15.6	515	1023	.36
1055	16.7	463	1022	.34
1155	18.3	515	1021	.32
1255	18.9	772	1021	.30
1355	19.4	412	1020	.31
1455	20.6	669	1019	.31
1555	21.1	566	1018	.31
1655	21.1	566	1018	.31
1755	20.6	566	1018	.31
1855	18.3	463	1017	.34
1955	16.1	463	1018	.41
2055	15.6	463	1018	.44
2155	14.4	463	1019	.47
2255	12.8	412	1019	.53
2355	12.8	257	1019	.53
Mean	**13.9**	**431**	**1020**	**.50**

TABLE 3.—*Land use characteristics*
[Source: Lewis and Outcalt (1976)]

Land use Type	ALB (percent)	SRHF (percent)	Z_0 (cm)	SILRAT
Low density residential (*LDR*)	0.18	0.60	73	0.13
Medium density residential (*MDR*)	.18	.30	86	.19
High density residential (*HDR*)	.14	.01	110	.19
Central business district (*CBD*)	.15	.05	400	.22
Commercial (*COMM*)	.15	.05	78	.02
Transportation (*TRANS*)	.15	.15	6	.02
Parks — Urban (*PARKS*)	.23	.90	80	.17

in the USGS-National Aeronautics and Space Administration study (Alexander and others, 1976) and were reported in Lewis and Outcalt (1976).

Although the category names may connote specific images of land use, these categories should not be interpreted too literally. For instance, the medium-density residential category specified by Lewis had a roughness length of 86 cm and a silhouette ratio of 0.19. In contrast, Myrup and Morgan (1972) used respective values of 532 cm and a 0.50 ratio to describe the same category. The land use categories used in this study are, therefore, general labels assigned for evaluating the influence of the urban terrain parameters.

A clearer view of the relationships between the land use categories is provided in figure 6. Low density, medium density, and high-density residential, for example, are chiefly distinguished by differences in surface relative humidity. The commercial and central business district categories both have very little evaporative surface, but their height and roughness characteristics are clearly dissimilar.

Albedo was added as an urban terrain parameter primarily because it distinguishes natural surfaces from artificial surfaces. Vegetation, in general, tends to reflect much more radiation in the near infrared range than do nonvegetated surfaces (Sellers, 1965). This effect would tend to decrease the amount of energy absorbed, decreasing the surface temperature.

A simulation run, using the URBD model, for May 11, 1972, was made using the data in tables 1 and 2 in order to test the response of the model to changes in the urban terrain values. In addition, latitude was specified as 39.9° lat., precipitable water was 10.0 mm, and dust particles were given as 1.0 particles cm^{-3} (Lewis and Outcalt, 1976). An observed sky radiant temperature, *TSKY*, of −5° C was used rather than the common formula of $TSKY = T_m - 22°$ C. An emissivity of 1.0 was assumed throughout the model.

Sample output data for the simulation of the micrometeorological conditions on May 11, 1972, in the medium-density residential land use category are shown in tables 4 and 5. The first five columns on the left in table 4 repeat meteorological boundary conditions input from table 3. The five columns on the right show the results of the shortwave radiation calculations. The shortwave radiation flux on a horizontal surface outside the Earth's atmosphere is depicted as *EXT*. The sum of the *BEAM*, diffused, and backscattered radiation flux on a horizontal surface at the Earth's surface is denoted as *SUN*. The total shortwave radiation flux on a vertical surface normal to the solar azimuth angle is represented as *VERT*. The *TERRAIN* variable averages *SUN* and *VERT* by considering the silhouette ratio and amount of area in shadow. The energy balance equation components for each time interval (3600 sec in this case) and the equilibrium surface temperature are listed in table 5.

At 0700 (solar time), for example, the model calculates that 344 W/m^{-2} of total shortwave radiation fall on a horizontal surface in Baltimore and 759 W/m^{-2} strike a vertical surface facing the sun. Since the silhouette ratio of vertical to horizontal surfaces for medium-density residential is 0.19, the vertical surface flux does not contribute significant energy to the overall average shortwave radiation flux of 344 W/m^{-2}. At this hour, the net radiation flux (R_n) is 243 W/m^{-2} due to the sunlight and rapidly increasing air temperature. Heat is being conducted into the soil (away from the surface) at a rate of −243 W/m^{-2} while the sensible heat flux to the air is −167 W/m^{-2}, indicating that convection is removing heat from the surface. Evaporative heat flux (LE) is still positive, 166 W/m^{-2}, indicating that heat is being added to the surface as water vapor condenses, forming dew.

Graphs of the simulated surface temperatures, as calculated from the standard run for each land-use category, are presented in figure 7. Driven by the four meteorological variables listed in table 2 at each time step, the URBD model computes the hourly temperatures as the curves labeled "H." The input variable reading procedure in the model was modified to use the 24-hour temperature average for the four meteorological variables instead of observed hourly values. The curve labeled "D" shows the resulting surface temperature.

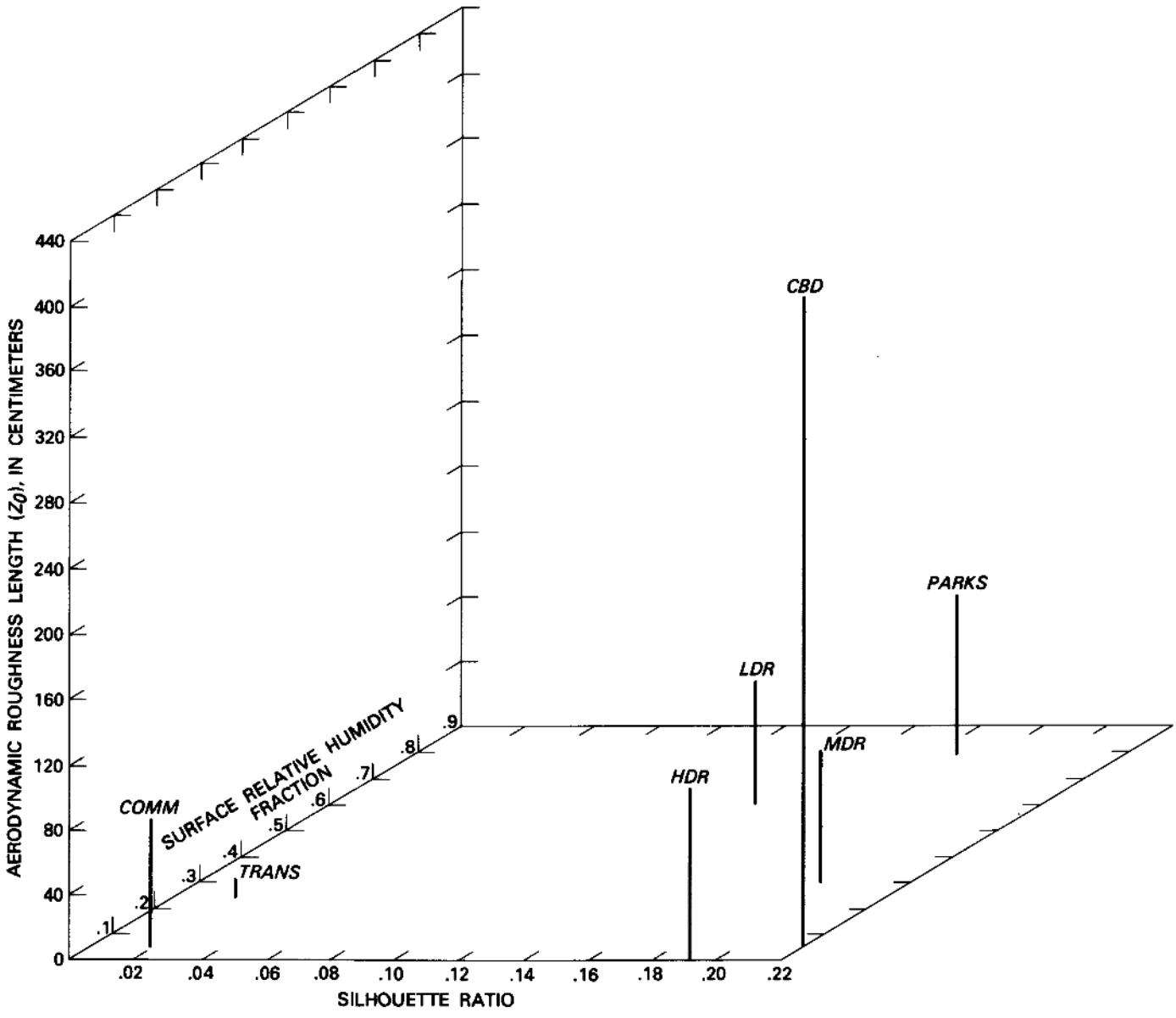

FIGURE 6.—Site characteristics for seven land use types.

ANALYSIS OF THE MODEL

When the simulations of surface temperature have been completed, the effectiveness of the URBD model can be evaluated by answering the following questions:

1. Is there a difference between driving the model with mean daily values for air temperature, relative humidity, wind speed, and air pressure, and driving the model at each time step?
2. How sensitive is the model to changes in the urban terrain parameters?
3. How do the simulated surface temperatures compare with observed results?

The seven standard runs of the URBD model, shown in figure 7, illustrate the differences between surface temperatures calculated with observed-hourly-value input and daily-near-value input. The daily input curves are relatively smooth and symmetrical around solar noon. The symmetry is not surprising, since energy is being added and subtracted from the model by net radiation. The daily input model also generates curves with shallow ranges, compared to the 20° C changes in the hourly input model. In addition, the maximum surface temperatures of hourly input lag behind the daily input model by two to three hours.

To determine the underlying causes for these

TABLE 4.—*Simulation of solar radiation flux for medium-density residential land use, May 11, 1972, Baltimore, Md.*

[Latitude=39.9° Soil thermal diffusivity=0.015 Solar declination=17.6° Time increments=3600
Month=5 Precipitable water (mm)=10.0 Day of the month=11 Dust particles (cm^{-3})=1.0
Soil wet fraction=0.30 Silhouette ratio=0.19 Albedo=0.19 Roughness length (cm=86]

Solar time	T_{air} (°C)	μ (cm sec^{-1})	p (mb)	RH	(Radiation values, in W/m^{-2}) EXT	BEAM	SUN	VERT	TERRAIN
0.00	7.2	360	1021	0.60	0	0	0	0	0
1.00	7.8	309	1021	.56	0	0	0	0	0
2.00	5.6	257	1021	.60	0	0	0	0	0
3.00	5.6	257	1021	.60	0	0	0	0	0
4.00	4.4	309	1021	.64	0	0	0	0	0
5.00	5.0	257	1022	.67	6	0	3	3	3
6.00	6.3	206	1023	.65	265	101	144	556	162
7.00	12.8	309	1023	.55	524	291	344	759	344
9.00	15.0	575	1023	.41	765	491	554	786	537
9.00	15.6	575	1023	.36	972	671	729	722	697
10.00	16.7	463	1022	.34	1131	812	872	609	807
11.00	18.3	515	1021	.32	1231	901	970	494	865
12.00	18.9	772	1021	.30	1307	932	994	440	883
13.00	19.4	412	1020	.31	1231	902	963	494	866
14.00	20.6	669	1019	.31	1131	812	873	610	807
15.00	21.1	566	1018	.31	972	671	731	723	699
16.00	21.1	566	1018	.31	765	492	549	831	538
17.00	20.6	566	1018	.31	524	292	344	761	345
18.00	18.3	463	1017	.34	265	101	145	559	162
19.00	16.1	463	1018	.41	6	0	3	3	3
20.00	15.6	463	1018	.44	0	0	0	0	0
21.00	14.4	463	1019	.47	0	0	0	0	0
22.00	12.8	412	1019	.53	0	0	0	0	0

model differences, the data were analyzed using a variation of the Students' *t*-test as described by Outcalt (1972a). The maximum surface temperatures, taken from the graphs, were regressed against four of the urban terrain parameters in two multiple-linear regression models: one for the daily mean value input, and one for the hourly observed value input. The Students' *t*-test was then used to compare the slope (*b* value) for a parameter in one model with the slope for the same parameter in the other model. When the slopes are significantly different, it can be inferred that the action of the test terrain parameter in both models helped create the resulting differences in surface temperature. The results of this test, applied to both daily maximum temperatures and temperature ranges, are listed in table 6.

TABLE 5.—*Simulation of micrometeorological conditions for medium-density residential land use, May 11, 1972, Baltimore, Md.*

Solar Time	(W/m^{-2}) R_n	S	H	LE	T_{surf} (°C)
0.00	−84	−77	−69	222	8.4
1.00	−83	−55	−39	178	8.6
2.00	−81	−47	−29	157	6.3
3.00	−81	−47	−29	157	6.3
4.00	−81	−63	−45	188	5.4
5.00	−79	−66	−41	185	6.0
6.00	72	−156	−82	167	10.7
7.00	243	−243	−167	166	16.5
8.00	434	−238	−246	50	18.7
9.00	592	−265	−273	−54	19.7
10.00	697	−303	−283	−112	21.3
11.00	755	−292	−297	−165	22.8
12.00	777	−232	−320	−225	22.5
13.00	753	−310	−264	−179	24.2
14.00	699	−230	−281	−188	24.1
15.00	591	−211	−227	−153	24.4
16.00	434	−159	−171	−105	23.6
17.00	246	−95	−103	−49	22.0
18.00	69	−58	−54	43	19.2
19.00	−87	−40	−37	166	16.7
20.00	−91	−56	−54	201	16.4
21.00	−91	−70	−66	227	15.5
22.00	−90	−89	−77	256	14.1
23.00	−89	−66	−36	185	13.7

The similarity of the maximum temperatures observed in figure 7 suggests that there were no significant model differences caused by the terrain parameters, and the *t*-test confirms this. All eight test statistics for (H-D)/S.E.(H) and (H-D)/S.E.(D) fall below the critical region. It is surprising, though, that the large differences in range cannot be attributed to any of the variables tested. Despite diurnal range differences of up to 20° C, the test statistics were even smaller than in the test on maximum surface temperature.

The next step was to examine the sensitivity of the hourly input model to changes in the terrain parameters. Sensitivity testing of a model can be approached several ways. At one extreme, the model can be subjected to large perturbations in parameter values and the temperature responses can then be examined. At the other extreme, parameter values can be changed by the potential experimental measurement error (Myrup and Morgan, 1972).

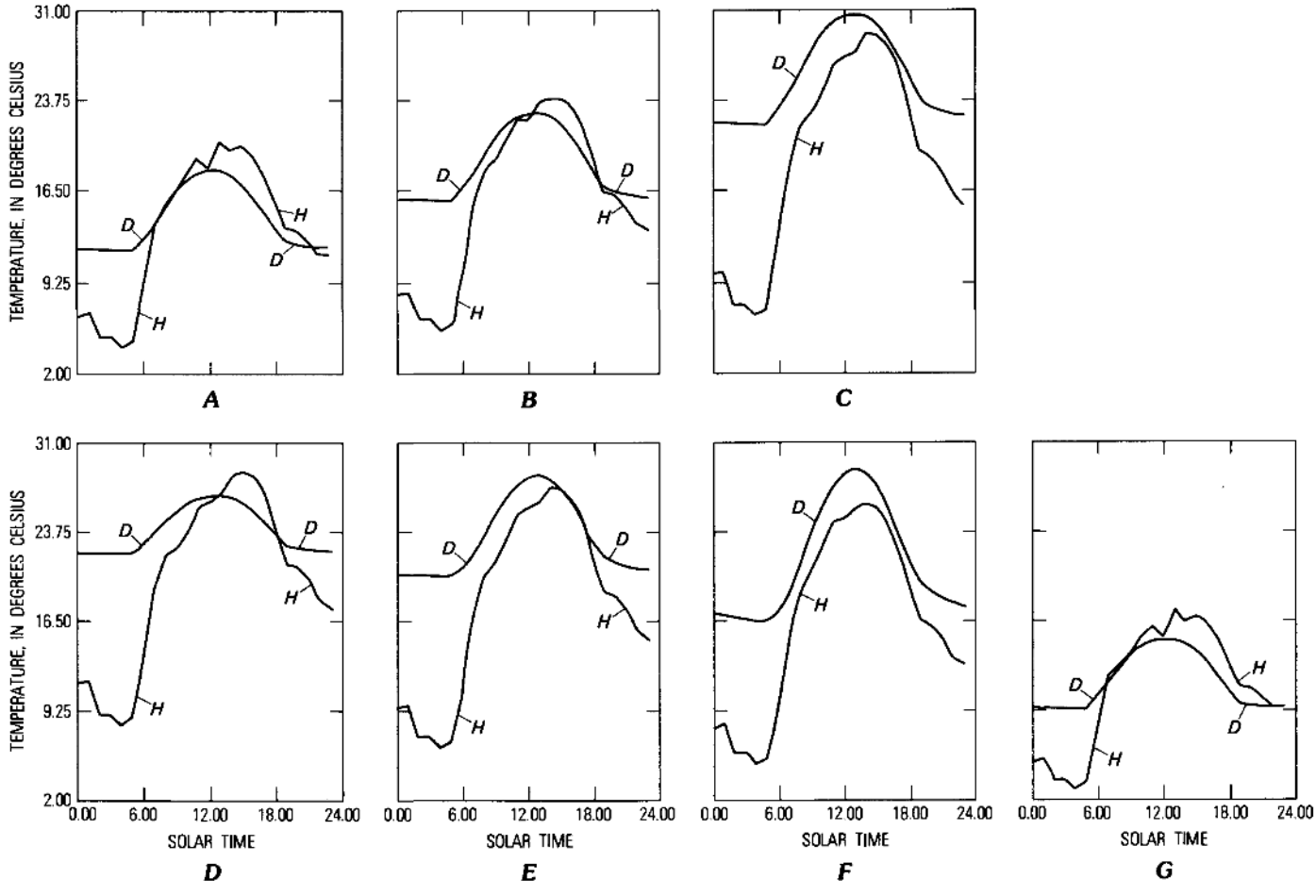

FIGURE 7.—Simulated surface temperatures in Baltimore, Md., for various land use categories based on hourly and averaged daily values on May 11, 1972. H indicates meteorological variables input hourly; D indicates meteorological variables input daily. *A*, Low-density residential. *B*, Medium-density residential. *C*, High-density residential. *D*, Central business district. *E*, Commercial land use. *F*, Transportation land use. *G*, Parks—urban land use.

In climate simulation, it is often meaningless to have large perturbations in just one variable since such a change is normally correlated with changes in a number of other variables. In this study, a middle ground between the extremes was sought by increasing and decreasing terrain parameter values by 30 percent.

The control run temperatures for 0500 and 1300 hours, using the land use input data described previously, are shown in table 7. Each of the parameters, *ALB*, h_o, *SILRAT*, κ, and *SRHF* were then altered by 30 percent, while all other variables were kept equal to their control run values. The results of these tests are listed in tables 8–12 and summarized in table 13.

Very little change in surface temperatures can be discerned from the data at 1300. The overall average deviation from the control temperature is $\pm 0.53°$ C. The maximum deviation, $-2.7°$ C, occurred when *SRHF*×1.3 was applied to the category *PARKS*. Over this range of perturbation, all five parameters acted linearly, causing temperatures to vary as much above the control values as below. Compare, for example, the columns labeled "$T_{surf}-T_c$", at 1300 in table 10. A 30 percent decrease in *SRHF* creates a temperature change with the same magnitude, but opposite direction, as a 30 percent increase in *SRHF*.

Overall, changes in *SRHF* caused the largest temperature changes. Looking at the tables, it is clear that changes in *SRHF* had the greatest effect on those land use types with high *SRHF* values. Conversely, κ had the most influence on those land use types with low *SRHF* values.

The results at 0500 are not as easily explained. In almost all tests, both increased and decreased

TABLE 6.—*Significance test for differences between URBD model using observed hourly data and mean daily data as input*

	b_{ALB}	b_{SRHF}	b_{TQ}	b_{SHUM}
Maximum surface temperature				
Hourly values (H)	—16.0	—12.6	0.002	2.3
Daily values (D)	—19.4	—16.1	—.007	.2
Standard error, S.E. (H)	43.7	4.1	.009	6.5
Standard error, S.E. (D)	92.4	8.6	.009	13.8
(H-D)/S.E. (H)	.08	.9	2.25	.32
(H-D)/S.E. (D)	.04	.4	1.0	.15
Diurnal temperature range				
Hourly values (H)	—14.8	—8.0	—0.004	—1.7
Daily values (D)	—29.6	—1.9	—.01	—5.3
Standard error, S.E. (H)	53.7	5.0	.005	8.0
Standard error, S.E. (D)	92.3	8.6	.009	13.8
(H-D)/S.E. (H)	.28	—1.22	1.2	.45
(H-D)/S.E. (D)	.16	—.71	.67	.26

parameter values caused a slight increase in temperature. The only exceptions were those land use types which had an extreme value for the parameter being tested. Although the model appears to be ignoring the magnitude of the change in each parameter, it is more likely that the change does not have a linear effect on the energy-balance components. By 0500, the surface temperature had a number of hours to come to equilibrium with T_{air} and $T2$ in the absence of additional radiation. Since the signs of the values $T_{air} - T_{surf}$ and $T2 - T_{surf}$ control the direction of flux, the components could be particularly sensitive.

The results of the test for differences between the hourly input model and the daily input model, and the sensitivity tests suggest that changes in individual urban terrain parameters have very little impact on the URBD model. The wide diurnal range of surface temperatures observed in figure 7, discussed earlier, suggests that wind speed and air temperature may be quite influential. Since hourly values for both wind speed and air temperature more than doubled over the course of May 11, 1972, such dynamic atmospheric conditions represent a realistic test of the model.

TABLE 7.—*Control run values of the URBD model for use in sensitivity testing.*

[T_c is the control run temperature]

Land use	T_c (°C)	
	0500	1300
LDR	4.6	20.8
MDR	6.0	24.2
HDR	7.5	29.0
CBD	9.1	27.9
COMM	6.8	27.5
TRANS	5.0	27.1
PARKS	3.1	17.4

The response of the model to large changes in wind speed is shown in tables 14 and 15. By examining the temperature change between $\mu\times0.25$ and $\mu\times0.50$ and comparing it to the change between $\mu\times1.5$ and $\mu\times2.0$, one can conclude that the model is more sensitive to changes in wind speed at low velocities. Land use types with little evaporative surface area, such as *HDR*, *CDB*, and *COMM*, however, showed very little response to changes in speed. The test of the model response to changes in air temperature was combined with the verification of the model so the two will be discussed simultaneously.

Observed radiant surface temperatures at 1400 e.s.t. for Baltimore on May 11, 1972, are shown in table 16. These values were corrected temperatures obtained from the ERIM thermal scanner data (Lewis, Outcalt, and Pease, 1975). As shown in figure 8, the model consistently underpredicts. Since the average deviation from the line of perfect prediction is −14° C, 14° C was added to each hourly air temperature, and the model was rerun. By adding 14° C, the average hourly temperature

TABLE 8.—*Sensitivity of the URBD model to changes in substrate diffusivity (κ)*

[Temperatures in degrees Celsius]

Land use	$\kappa\times0.7$				$\kappa\times1.3$			
	0500		1300		0500		1300	
	T_{surf}	$T_{surf}-T_C$	T_{surf}	$T_{surf}-T_C$	T_{surf}	$T_{surf}-T_C$	T_{surf}	$T_{surf}-T_C$
LDR	5.0	0.4	20.9	0.1	5.0	0.4	20.7	−0.1
MDR	6.6	.6	24.8	.6	6.2	.2	23.7	−.5
HDR	8.4	.9	30.8	1.8	7.3	−.2	27.6	−1.4
CBD	9.8	.7	28.8	.9	8.8	−.3	27.1	−.8
COMM	7.6	.8	29.0	1.5	6.8	.0	26.3	−1.2
TRANS	5.7	.7	28.9	1.8	5.4	.4	25.7	−1.4
PARKS	3.3	.2	17.3	−.1	3.6	.5	17.5	.1

TABLE 9.—*Sensitivity of the URBD model to changes in the height of obstructions (h_o)*
[Temperatures in degrees Celsius]

Land use	$h_o \times 0.7$				$h_o \times 1.3$			
	0500		1300		0500		1300	
	T_{surf}	$T_{surf}-T_C$	T_{surf}	$T_{surf}-T_C$	T_{surf}	$T_{surf}-T_C$	T_{surf}	$T_{surf}-T_C$
LDR	4.9	0.3	21.4	0.6	5.0	0.4	20.3	−0.5
MDR	6.2	.2	24.6	.4	6.5	.5	23.8	−.4
HDR	7.4	−.1	28.9	−.1	8.0	.5	29.0	.0
CBD	8.7	−.4	27.9	.0	9.6	.5	27.8	−.1
COMM	6.9	.1	27.5	.0	7.4	.6	27.4	−.1
TRANS	5.4	.4	27.1	.0	5.6	.6	26.9	−.2
PARKS	3.5	.4	18.1	.7	3.5	.4	16.8	−.6

TABLE 10.—*Sensitivity of the URBD model to changes in the surface relative humidity fraction (SHRF)*
[Temperatures in degrees Celsius]

Land use	SRHF ×0.7				SRHF ×1.3			
	0500		1300		0500		1300	
	T_{surf}	$T_{surf}-T_C$	T_{surf}	$T_{surf}-T_C$	T_{surf}	$T_{surf}-T_C$	T_{surf}	$T_{surf}-T_C$
LDR	5.7	1.1	22.8	2.0	4.1	−0.5	18.9	−1.9
MDR	6.7	.7	25.4	1.2	6.0	.0	23.0	−1.2
HDR	7.8	.3	29.0	.0	7.7	.2	28.9	−0.1
CBD	9.4	.3	28.3	.4	9.1	.0	27.4	−.5
COMM	7.2	.4	27.7	.2	7.1	.3	27.2	−.3
TRANS	5.6	.6	27.2	.1	5.5	.5	26.7	−.4
PARKS	4.9	1.8	20.1	2.7	1.8	−1.3	14.7	−2.7

TABLE 11.—*Sensitivity of the URBD model to changes in silhouette ratio (SILRAT)*
[Temperatures in degrees Celsius]

Land use	SILRAT ×0.7				SILRAT ×1.3			
	0500		1300		0500		1300	
	T_{surf}	$T_{surf}-T_C$	T_{surf}	$T_{surf}-T_C$	T_{surf}	$T_{surf}-T_C$	T_{surf}	$T_{surf}-T_C$
LDR	4.9	0.3	21.3	0.5	5.0	0.4	20.4	−0.4
MDR	6.1	.1	24.4	.2	6.5	.5	24.0	−.2
HDR	7.3	−.2	28.7	−.3	8.1	.6	29.2	.2
CBD	8.7	−.4	27.8	−.1	9.7	.6	27.9	.0
COMM	6.8	.0	27.4	−.1	7.4	.6	27.5	.0
TRANS	5.4	.4	27.0	−.1	5.6	.6	26.9	−.2
PARKS	3.5	.4	18.0	.6	3.5	.4	17.0	−.4

TABLE 12.—*Sensitivity of the URBD model to changes in albedo (ALB)*
[Temperatures in degrees Celsius]

Land use	ALB ×0.7				ALB ×1.3			
	0500		1300		0500		1300	
	T_{surf}	$T_{surf}-T_C$	T_{surf}	$T_{surf}-T_C$	T_{surf}	$T_{surf}-T_C$	T_{surf}	$T_{surf}-T_C$
LDR	5.0	0.4	21.1	0.3	5.0	0.4	20.5	−0.3
MDR	6.3	.3	24.5	.3	6.3	.3	23.9	−.3
HDR	7.8	.3	29.2	.2	7.8	.3	28.7	−.3
CBD	9.3	.2	28.0	.1	9.3	.2	27.7	−.2
COMM	7.1	.3	27.7	.2	7.1	.3	27.2	−.3
TRANS	5.5	.5	27.4	.3	5.5	.5	26.6	−.5
PARKS	3.5	.4	17.8	.4	3.5	.4	17.0	−.4

TABLE 13.—*Rank (R) of absolute value of $T_{surf}-T_C$ at 1300 for each land use type*
[Temperature value is the average of parameter×0.7 and parameter×1.3]

Parameter	LDR		MDR		HDR		CBD		COMM		TRANS		PARKS	
	°C	(R)	°C	(R)	°C	(R)	°C	(R)	°C	(R)	°C	(R)	°C	(R)
SRHF	1.95	(1)	1.20	(1)	0.05	(3)	0.45	(2)	0.25	(2)	0.25	(3)	2.70	(1)
h_o	.55	(2)	.40	(3)	.05	(3)	.00	(5)	.05	(3)	.10	(5)	.65	(2)
SILRAT	.45	(3)	.20	(5)	.25	(2)	.05	(4)	.05	(3)	.15	(4)	.50	(3)
ALB	.30	(4)	.30	(4)	.25	(2)	.15	(3)	.25	(2)	.40	(2)	.40	(4)
K	.10	(5)	.55	(2)	1.60	(1)	.85	(1)	1.35	(1)	1.60	(1)	.10	(5)

TABLE 14.—*Sensitivity of the URBD model to decreased wind speed (μ)*

[Temperatures in degrees Celsius]

Land use	$\mu \times 0.25$				$\mu \times 0.50$			
	0500		1300		0500		1300	
	T_{surf}	$T_{surf}-T_C$	T_{surf}	$T_{surf}-T_C$	T_{surf}	$T_{surf}-T_C$	T_{surf}	$T_{surf}-T_C$
LDR	4.6	0.0	25.4	4.6	4.8	0.2	23.1	2.3
MDR	5.4	−.6	26.9	2.7	5.8	−.2	25.6	1.4
HDR	6.0	−1.5	28.8	−.2	6.8	−.7	28.8	−.2
CBD	7.4	−1.7	28.2	.3	8.4	−.7	28.0	.1
COMM	5.7	−1.1	27.5	.0	6.3	−.5	27.5	.0
TRANS	4.8	−.2	27.8	.7	5.1	.1	27.5	.4
PARKS	3.6	.5	23.1	5.7	3.5	.4	20.0	2.6

TABLE 15.—*Sensitivity of the URBD model to increased wind speed (μ)*

[Temperatures in degrees Celsius]

Land use	$\mu \times 1.5$				$\mu \times 2.0$			
	0500		1300		0500		1300	
	T_{surf}	$T_{surf}-T_C$	T_{surf}	$T_{surf}-T_C$	T_{surf}	$T_{surf}-T_C$	T_{surf}	$T_{surf}-T_C$
LDR	5.1	0.5	19.6	−1.2	5.1	0.5	18.9	−1.9
MDR	6.7	.7	23.4	−.8	6.9	.9	22.9	−1.3
HDR	8.4	.9	29.0	.0	8.9	1.4	29.0	.0
CBD	9.7	.6	27.7	−.2	10.1	1.0	27.7	−.2
COMM	7.8	1.0	27.4	−.1	8.2	1.4	27.4	−.1
TRANS	5.9	.9	26.6	−.5	6.2	1.2	26.4	−.7
PARKS	3.4	.3	16.1	−1.3	3.4	.3	15.3	−2.1

TABLE 16.—Comparison of observed and simulated surface temperature, 1400 EST, May 11, 1972 (in degrees celsius)

[Control run: r=0.95, $b1$=0.62, I air+14°C: r=0.95, $b1$=1.09 (Lewis and others, 1975)]

Land use	T_{surf}		
	Observed	Simulated (Control)	Simulated (T_{air} + 14°C
LDR	32.9	20.8	31.4
MDR	40.0	24.2	37.1
HDR	47.9	29.0	47.4
COMM	40.0	27.5	44.2
TRANS	40.0	27.1	40.0
PARKS	28.0	17.4	26.7

TABLE 17.—*Simulation of global incoming solar radiation*

[Measured on the parking lot at the State fairgrounds, Timonium, Md., on May 11, 1972 (Lewis and others, 1975)]

Time (solar)	Radiation (W/m^{-2})	
	Measured	Simulated
0600	84	141
0700	286	338
0800	481	541
0900	725	722
1000	809	865
1100	941	955
1200	997	986
1300	955	955
1400	851	865
1500	662	724

was doubled. The resulting surface temperatures average 55 percent higher than the control temperatures (see table 16).

This second set of predicted temperatures is much closer to the observed values than those of the control run. If surface temperature was a linear function of air temperature, the slope of the regression line for the control data would be expected to be the same as the slope for the $T_{air}+14°$ C data. These two slopes are 0.62 for the control run and 1.09 for the increased air temperature. Unfortunately, there are not sufficient degrees of freedom to test the hypothesis that the two slopes are equal.

A secondary check on the model is provided by global radiation data collected at Timonium, Md., on May 11, 1972, (Lewis, Outcalt, and Pease, 1975). The location of Timonium, about 12 miles north of Baltimore, is depicted in figure 5. The observed data shown in table 17 compares quite closely to simulated global radiation, particularly between 0900 and 1400. The maximum deviation between those hours is 6.9 percent.

CONCLUSION

The application of an energy-balance simulation model to urban area analyses requires recognition of the tremendous variety of surfaces, heights, orientations, densities, and materials found in a city. Although sensitivity analysis demonstrates that changes on the order of 30 percent, in individual urban terrain parameters, have relatively little effect on surface temperatures, the effects can be

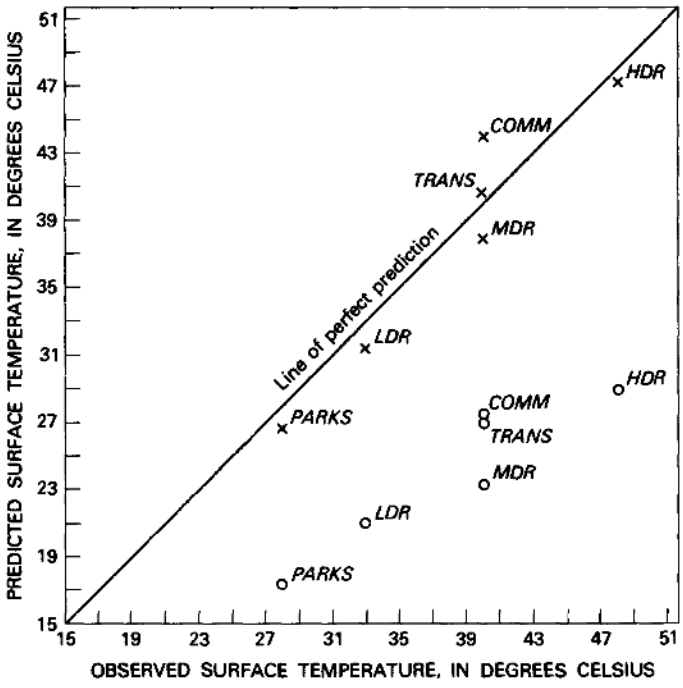

FIGURE 8.—Effect of increased air temperature on the predicted surface temperature. Control run values represented by a small circle and $T_{air} + 14°C$ values by an x.

multiplied when more than one parameter are considered. The seven different land use types, specified by the urban terrain variables, had varied responses to the same meteorological boundary conditions.

This result suggests that further work in analyzing the URBD model could start by using each of the three-dimensional cells of figure 6 as a unique "land use." One could then test the surface-temperature response to changes in three linked parameters rather than just one.

The comparison of the hourly observed-value input model with the daily mean-value input model demonstrates the advantage of time dependent values for wind speed and air temperature. The significant differences suggest that the effects of changes in air relative humidity should also be tested. Although the use of an average air temperature did not appear to seriously affect the surface temperatures around midday, the consequences appear to be more serious at night. In the absence of any shortwave radiation, air with a temperature much warmer than the ground temperature provides a major source of heat to the system.

The sensitivity of the model to air temperature and wind speed calls into question the use of uniform meteorological boundary conditions for all land use types. Characteristically, temperatures throughout a city are not uniform 6 feet off the ground. Since this value exerts such strong control on the sensible heat flux to the air and evaporative heat flux, its specification should be carefully studied.

While the predictive value of the URBD model was deemphasized in this study, the goal of accurately simulating urban meteorological processes provides the impetus for modeling urban climates. In some ways, the fortuitous results of the first attempt to verify an urban simulator (Outcalt, 1972a and 1972b) may have misled investigators. The fact that Outcalt's simulated temperatures were within 1.5° C of observed temperatures at Ann Arbor, Mich., belies the complex energy exchange processes occurring in a city. A unique surface temperature occurs for a given set of energy fluxes, but an observed surface temperature can result from a numerous set of urban terrain parameters from which the four components of the energy balance equation are calculated. It should also be pointed out, though, that Baltimore is a larger, more complex site than Ann Arbor. In addition, the potential climatic effects of Chesapeake Bay are ignored by the one-dimensional URBD model.

In this case, the real benefit of an urban climate simulator lies not in the predicted values but in the ability to examine relationships between components. An understanding of the sensitivity of the model, in turn, can be used to improve simulation techniques and field verification.

REFERENCES CITED

Alexander, R. A., Lewis, J. E., Lins, H. F., Jenner, C. B., Outcalt, S. I., and Pease, R. W., 1976, Application of Skylab data to land use and climatological analysis: Final Report SKLAB/EREP Investigation No. 469, 210 p.

Bornstein, R. D., 1968, Observations of the urban heat island effect in New York City: Journal of Applied Meteorology, v. 7, no. 4, p. 575–582.

——— 1975, The two-dimensional URBNET urban boundary layer model: Journal of Applied Meteorology, v. 14, no. 8, 1459–1477.

Gutman, D. P. and Torrance, K. E., 1975, Response of the urban boundary layer to heat addition and surface roughness: Boundary Layer Meteorology: v. 9. no. 2, p. 217–233.

Hage, K. D., 1975, Urban-rural humidity differences: Journal of Applied Meteorology, v. 14, no. 7, 1277–1283.

Leahey, D. M. and Friend, J. P., 1971, A model for predicting the depth of the mixing layer over an urban heat island with application to New York City: Journal of Applied Meteorology, v. 10, no. 6, p. 1162–1173.

Lettau, H., 1969, Note on aerodynamic roughness parameter estimation on the basis of roughness element description:

Journal of Applied Meteorology, v. 8, p. 828–832.

Lewis, J. E., and Outcalt, S. I., 1976, Verifying an urban surface climate simulation model: paper submitted to be read at the International Geographical Union held in Moscow, July–August, 1976.

Lewis, J. E., Outcalt, S. I., and Pease, P. W., 1975, urban surface thermal response associated with land use: unpublished paper presented at the Symposium on Meteorology as Related to Urban and Regional Land-Use Planning, Asheville, North Carolina, November 1975.

Marotz, G. A. and Coiner, J. C., 1973, Acquisition and characteristics of surface material data for urban climatological studies: Journal of Applied Meteorology, v. 12, no. 6, p. 919–923.

McElroy, J. L., 1973, A numerical study of the nocturnal heat island over a medium-sized mid-latitude city (Columbus, Ohio): Boundary Layer Meteorology, v. 3, p. 442–453.

Myrup, L. O., 1969, A numerical model of the urban heat island: Journal of Applied Meteorology, v. 8, no. 6, p. 908–918.

Myrup, L. O., and Morgan, D. L., 1972, A numerical model of the urban atmosphere: Contributions in Atmospheric Science, v. 1, no. 4, University of California at Davis, 237 p.

Outcalt, S. I., 1972a, A reconnaissance experiment in mapping and modeling the effect of land use on urban thermal regimes: Journal of Applied Meteorology, v. 11, no. 8, p. 1369–1373.

——— 1972b, A synthetic analysis of seasonal influences in the effects of land use on the urban thermal regime: Archiv für Meteorologie, Geophysik und Bioklimatologie, ser. A, v. 20, p. 253–260.

Outcalt, S. I., and Carlson, J., 1975, A coupled soil thermal regime surface energy budget simulator: Conference on Soil Water Problems in Cold Regions, Calgary, Canada, proceedings, 211 p.

Schneider, S. H. and Dickinson, R. E., 1974, Climate modeling: Review of geophysics and space physics, v. 12, no. 3, p. 447–493.

Sellers, W. D., 1965, Physical Climatology: Chicago, University of Chicago Press, 272 p.

Terjung, W. H., 1970, Urban energy balance climatology: Geographical Review, v. 60, no. 1, p. 31–53.

Terjung, W. H. and Collaborators, 1970, The energy-balance climatology of a city-man system, Annals Association of American Geographers, v. 60, no. 3, p. 466–492.

Tuller, S. E., 1973, Microclimatic variations in a downtown urban environment: Geografiska Annaler, v. 55A, no. 3, p. 123–136.

The Washington Post, Daily weather data, May 10–12, 1972.

Yu, T. W. and Wagner, N. K., 1975, A numerical study of the nocturnal urban boundary layer: Boundary Layer Meteorology, v. 9, no. 2, p. 143–162.

☆ U.S. GOVERNMENT PRINTING OFFICE: 1980 O— 311-344/131